Eur. Radiol. 8, 1558–1564 (1998)

European
Radiology

Original article

A new volumetric CT machine for dental imaging based on the cone-beam technique: preliminary results

P. Mozzo[1], **C. Procacci**[2], **A. Tacconi**[2], **P. Tinazzi Martini**[2], **I. A. Bergamo Andreis**[2]

[1] Department of Medical Physics, University Hospital, I-37134 Verona, Italy
[2] Department of Radiology, University Hospital, I-37134 Verona, Italy

Received 7 July 1997; Revision received 17 October 1997; Accepted 2 June 1998

Abstract. The objective of this paper is to present a new type of volumetric CT which uses the cone-beam technique instead of traditional fan-beam technique. The machine is dedicated to the dento-maxillo-facial imaging, particularly for planning in the field of implantology. The main characteristics of the unit are presented with reference to the technical parameters as well as the software performance. Images obtained are reported as various 2D sections of a volume reconstruction. Also, measurements of the geometric accuracy and the radiation dose absorbed by the patient are obtained using specific phantoms. Absorbed dose is compared with that given off by spiral CT. Geometric accuracy, evaluated with reference to various reconstruction modalities and different spatial orientations, is 0.8–1 % for width measurements and 2.2 % for height measurements. Radiation dose absorbed during the scan shows different profiles in central and peripheral axes. As regards the maximum value of the central profile, dose from the new unit is approximately one sixth that of traditional spiral CT. The new system appears to be very promising in dento-maxillo-facial imaging and, due to the good ratio between performance and low cost, together with low radiation dose, very interesting in view of large-scale use of the CT technique in such diagnostic applications.

Key words: Computed tomography – Cone beam – Dental imaging

Introduction

Computed tomography is routinely employed in the diagnosis and treatment planning of dental and maxillo-facial structures, with particular reference to dental implant surgery [1–5]. Special application software allows attainment of, by reformatting, 2D images perpendicular to the dental arch and panoramic views of the dental arch as well as 3D views. However, the cost and complexity of these machines, along with the problems related to the high dose absorbed by the patient, limit the use of this modality.

In this paper we present the preliminary results achieved with a new type of CT machine devoted to the imaging of dental and maxillo-facial structures and based on the cone-beam technique (CBCT).

The CBCT technique has been employed previously in radiotherapy, using fluoroscopic systems or modified simulators in order to obtain cross sections of the patient in the same geometric conditions of the treatment [6–11]. The CBCT technique has also been employed in vascular imaging and in micro-tomography of small specimens for biomedical and industrial applications. The technique seems to be very promising due to inherent quickness in volumetric acquisition and to high efficiency in X-ray use. Moreover, it permits intrinsically the manufacture of less expensive CT machines. Potential disadvantages are, however, the scattered radiation [12] and the limited dynamic range of the X-ray area detectors, based on the presently employed image intensifier tube and TV chain. Image intensifiers have also low diameters as regards CT applications; thus, "truncated-view" artifacts are also present [13].

The new machine presented in this paper is the first commercial CBCT system devoted to dento-maxillo-facial imaging.

Materials and methods

The new machine (NewTom-9000, Quantitative Radiology, Verona, Italy) uses a cone-shaped X-ray beam centered on an X-ray area detector (Fig. 1). The tube-detector system performs a complete 360° rotation around the head of the patient, during which a series of expo-

Correspondence to: P. Mozzo

Present address: Viale Caduti del Lavoro 7, I-37057 S.Giovanni Lupatoto, Verona, Italy

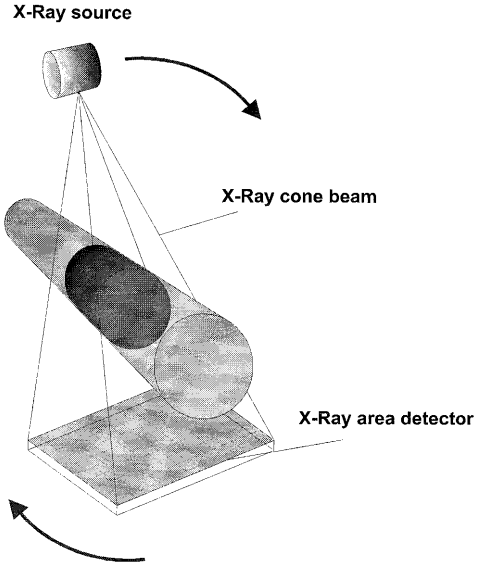

Fig. 1. Representation of the cone-beam technique

Table 1. Technical data of the scan

Reconstruction volume ($\Phi \times$ h)	15 × 15 cm
Scan angle	360°
Scan time	70 s
Effective exposure time	18 s
X-ray beam	Conic, pulsed
kV	110
mA (max.)	15
mAs/scan (typical)	100
X-ray area detector	400 cm^2, 262,000 pixels
Spatial resolution	0.3 mm in x, y, and z directions

sures (typically, one for each degree) is achieved which provides, as digital images, the raw data used for the reconstruction of the examined volume. The reconstruction volume is a cylinder 15 cm high with a diameter of 15 cm.

The X-ray beam is pulsed and synchronized with both the acquisition system and the scanner. The X-ray area detector is a special image intensifier (9") coupled with a solid-state (CCD) TV camera. Digital radiograms are acquired in a 512 × 512 format. The technical data on the scan as well as on the detector are summarized in Table 1.

The CBCT technique allows, in principle, obtainment of data acquisitions much faster than traditional CT. With the new machine the speed is limited by technological and economical factors. Presently, the scan time is 70 s, but in a few months it will probably be halved. The system, moreover, is particularly advantageous in using X-ray emission. In fact, in fan-beam techniques only a few thousandths (on average) of the produced beam is employed in producing images, and in the case of volumetric reconstruction it is necessary to produce n-times the X-photons used by CBCT (if n is the number of slices necessary to cover the volume of interest). Typically, with NewTom 100 mAs is needed for a complete scan of maxilla and mandible, and approximately 23,000 mAs (330 mAs per slice × 70 1-mm slices) are required for the same volume reconstruction with traditional CT. Low radiological power and low mechanical requirements, due to low scan speed, determine the manufacturing simplicity and low price of the new machine.

The system has an automatic exposure control (AEC) device which allows automatic selection of the starting intensity of the X-ray beam according to the size of the patient as well as modification of it while scanning according to the thickness of the traversed tissues. There is also a device to control the size of the beam and to limit the irradiated volume.

Problems due to limited dynamic range of the detector are overcome by using a special wedge-shaped circular filter which modulates properly the intensity of the incident beam, reducing the intensity on the borders with respect to the center, according to the approximately circular cross section of the head of the patient, thus reducing the dynamics of the transmitted beam.

Scattered radiation limits the signal-to-noise ratio (SNR), but the air gap between object and detector (30 cm long) is sufficient to obtain good improvement in SNR [14]; moreover, low-contrast resolution is not the main objective of the machine.

The main truncated-view artifact (circular edge on field borders) is partly hidden simply by visualizing regions smaller than the field of view. Distortion of CT numbers is of no interest in this context, since no quantitative analysis is presently performed.

The raw data are preliminarily corrected for geometrical and dynamic distortions of the detector and are then elaborated by a modified version of the 3D filtered back-projection method proposed by Feldkamp et al. [15].

The basic software allows obtainment of, by means of a primary (or direct) reconstruction, all axial slices enclosed in a given region chosen by the operator on one of the lateral views of the head used as scout view (taking the beam divergence into account). The slices may also be para-axial oblique, i.e., "tilted" vs the conventional axial planes (e.g., parallel to the base of the mandible). The contiguous slices may be 1 or 2 mm thick. Several primary reconstructions can be achieved with the raw data of a single scan, either on different planes or with different extension of the reconstructed region.

In Fig. 2 three para-axial oblique (or "tilted") images of the upper jaw of a patient are reported, reconstructed on planes shown in the corresponding scout view. Figure 3 shows three other tilted images reconstructed from the same raw data on planes parallel to the base of the mandible (as pointed out in the corresponding scout view). Ring artifacts observed in these images are caused by the not yet satisfying software system which compensates for inhomogeneity of CCD-pixel efficiency. Also visible are streak artifacts produced by undersampling, because the number of projections is slightly lower than that required to fully determine the reconstruction matrix.

No artifacts are evident, because of the divergence of X-ray beams, in planes different from mid-plane [15], probably because of small cone angles. From the axial

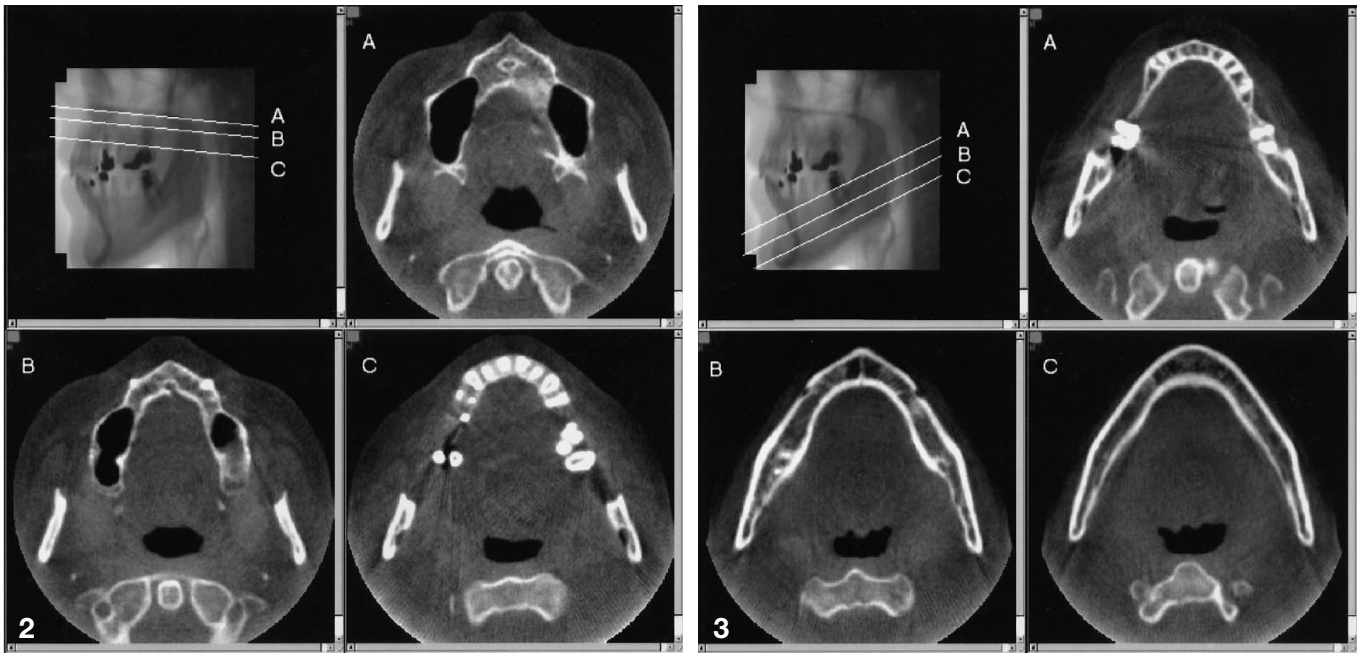

Fig. 2. Para-axial oblique (or tilted) images of the upper jaw with the corresponding scout view

Fig. 3. Para-axial oblique (or tilted) images of mandible reconstructed on planes parallel to the base of the mandible

or tilted images (primary reconstruction) it is possible to achieve, by means of reformattings called secondary reconstructions (multiplanar reformatting, MPR), 2D images perpendicular to the dental arch (PDA images), 2D panoramic images, and 3D views.

The 2D images are obtained by reformatting along planes perpendicular to those of the axial (or tilted) slices. They are created from arches of parabola positioned on one of the axial views of the dental arches. They encompass sequences of images achieved along planes perpendicular to the parabola (PDA images) and views corresponding to planes parallel to the parabola itself (panoramic images).

In Figs. 4–6 some examples of secondary reconstructions are reported, related to the same examination from which Figs. 2 and 3 are extracted. On all 2D images it is possible to measure the distances both manually, pointing with the mouse to the range of the evaluated segment, and automatically in cases of segments crossing two edges of bone soft tissue interface.

A special option of the software of the machine allows, by means of a colored marker, to point at an anatomical detail on a 2D view and to recover it automatically on all the other reformatted 2D slices. The option can be used, for example, to demonstrate the course of the mandibular canal (Fig. 7).

The machine has a Windows NT (Microsoft, Seattle, Wash.)-compatible workstation, with either Pentium (Intel, Santa Clara, Calif.), Indigo (Silicon Graphics, Mountain View, Calif.), or Alpha (Digital Equipment Corp., Maynard, Mass.) processors. With a 200-MHz P6 Intel processor, the primary reconstruction of 30 axi-

Fig. 4. Perpendicular-to-dental-arch images (PDA) of the mandible with corresponding tilted image of reference

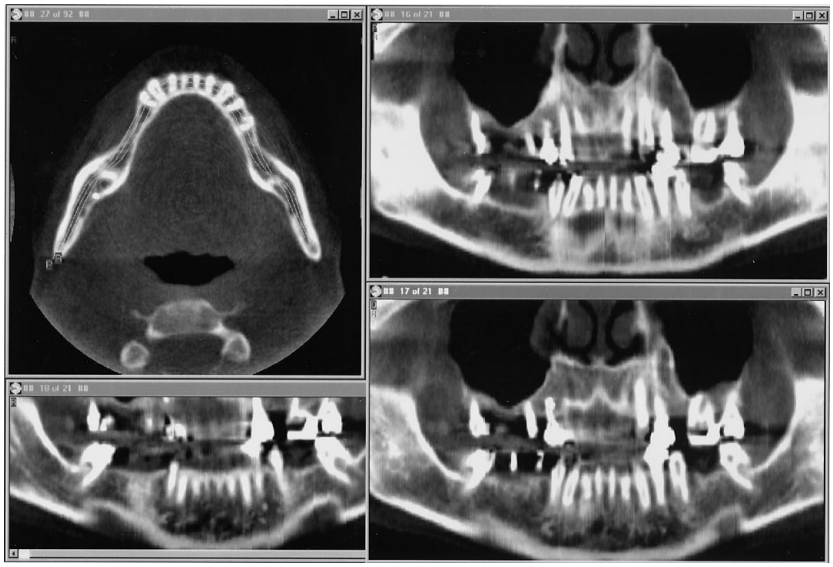

Fig. 5. Panoramic views of reconstructed region with the tilted image of reference

Fig. 6. Three-dimensional representations of the reconstructed region

al slices requires approximately 10 min. The secondary reconstructions are, on the contrary, done in real time.

Examinations were performed both on anthropomorphic phantoms and on patients. Informed consent was obtained before scanning the patients. Moreover, in order to assess the accuracy of the geometric measurements, exams were done on a geometric phantom which consisted of a polymethyl-metacrylate (PMMA) cylinder, 16 cm in diameter and 20 cm high, containing two concentric bone-equivalent plastic inserts (Fig. 8a) with the sizes summarized in Table 2. The inserts simulate schematically the cortical walls of a mandibular bone.

Table 2. Dimensions of the inserts used in the phantom for testing geometrical accuracy

Dimension	Insert 1 (internal circle)	Insert 2 (external circle)
Internal diameter (mm)	76.40	94.60
External diameter (mm)	82.10	100.60
Height (mm)	8.10	8.10

The absorbed dose was measured with passive thermoluminescence dosimeters (LiF-100). The detectors were inserted into a phantom similar to that used for the accuracy trials but without the inserts and with holes for holding TLD dosimeters. More precisely, these holes are positioned along lines parallel to the symmetry axis of the phantom, in its center and 10 cm from the surface (at 90° intervals; Fig. 8b) and separated between them 20 mm. Phantom characteristics are in accordance with those indicated for the head dosimetric phantom by the FDA (21 CFR 1020.39) and by IEC (601–2-44, part 2, in press). The scan of the phantom was done with the standard radiological parameters reported in Table 1 (100 mAs/scan). The X-ray beam was delimited in such a way that it was possible to reconstruct a 70-mm region. As a comparison, the same phantom underwent also a dental-scan exam with a conventional CT machine (Somatom Plus 4, Siemens, Erlangen, Germany), by means of 70 contiguous 1-mm-thick scans at 120 kV and 330 mAs.

Results

Geometric accuracy

The geometric accuracy was evaluated by means of the geometric phantom with the two circular inserts representative of the cortical walls of the mandibular bone. Two exams were done, one with the phantom in horizontal position (primary axial reconstruction), and the

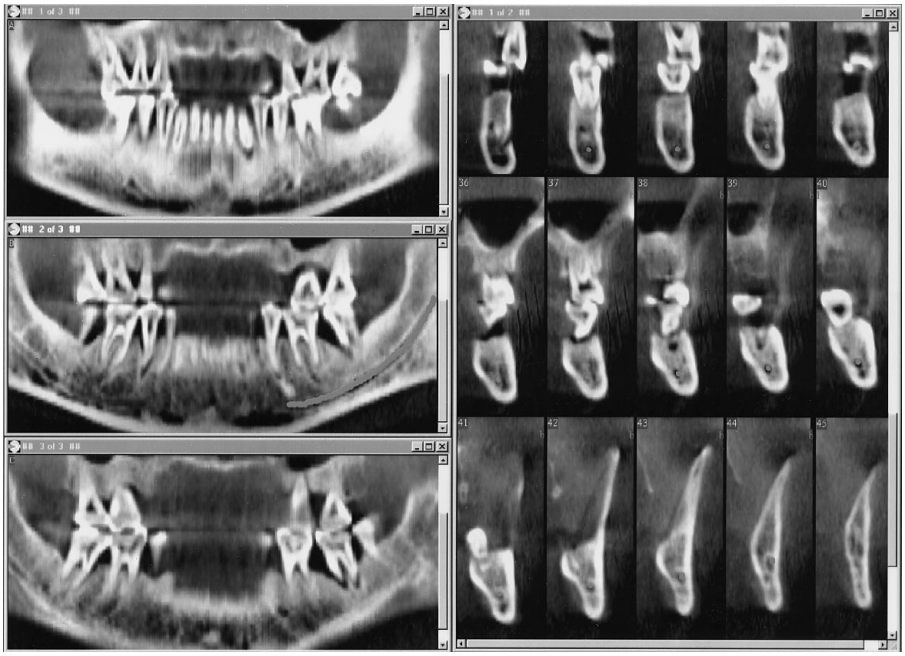

Fig. 7. Panoramic and PDA images from an anthropomorphic phantom study with the mandibular nerve marked in panoramics and, automatically, in PDA images

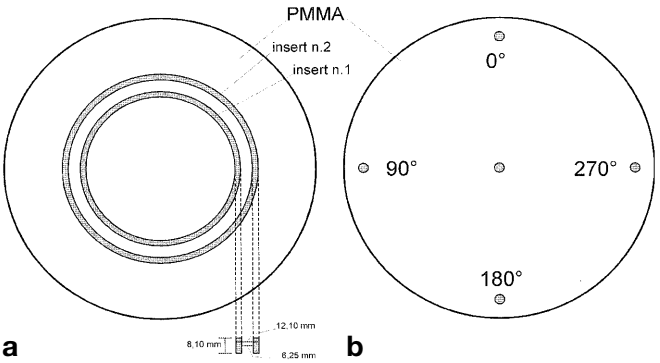

Fig. 8. Representation of the sections of the phantoms used for **a** testing geometrical accuracy and for **b** measuring the absorbed radiation dose. *PMMA* polymethyl-metacrylate

other with the phantom at a 30° angle (primary reconstruction with the same "tilt" angle). In both cases we measured with reference to the simulated mandibular bone: external and internal widths on axial or tilted images, external and internal widths as well as the height on PDA images, and height on panoramic views.

In order to carry out measurements independent from the observer, as much as was possible, the automatic option for measurements was used. With this option it is possible to select, using the mouse, a segment across the two bone soft tissue edges of interest, and then the software analyzes the corresponding densitometric profile (Fig. 9) setting automatically the bones' borders at half height of the edges.

All measurements were repeated at three different points, at 0, 90, and 270°. The mean value of the three measurements was considered. The results are shown in Table 3. The difference observed between the true value and general mean value was 0.8–1 % for width measurements and 2.2 % for height measurements.

The test demonstrates the good accuracy of the system with reference to all the possible spatial orientations of the reconstructed images. All images can be printed on a 1:1 scale. The accuracy of the measurements is one of the main targets of the system, mainly for pre-implant imaging.

Absorbed dose

The results of the dose measurements are shown as dose profiles, i. e., absorbed dose as function of position along lines of the phantom. For each measurement the five

Table 3. Results of the measurements on inserts of the phantom for testing geometrical accuracy. PDA perpendicular-to-dental-arch image

	External width (true value: 12.10 mm)	Internal width (true value: 6.25 mm)	Height (true value: 8.10 mm)
Axial (mm; tilt 0°)	12.00	6.40	–
Tilted (mm; tilt 30°)	12.08	6.32	–
PDA (mm; tilt 0°)	12.08	6.23	7.92
PDA (mm; tilt 30°)	11.75	6.25	8.00
Panoramics (mm; tilt 0°)	–	–	7.75
Panoramics (mm; tilt 30°)	–	–	8.00
General means (mm)	11.98	6.30	7.92

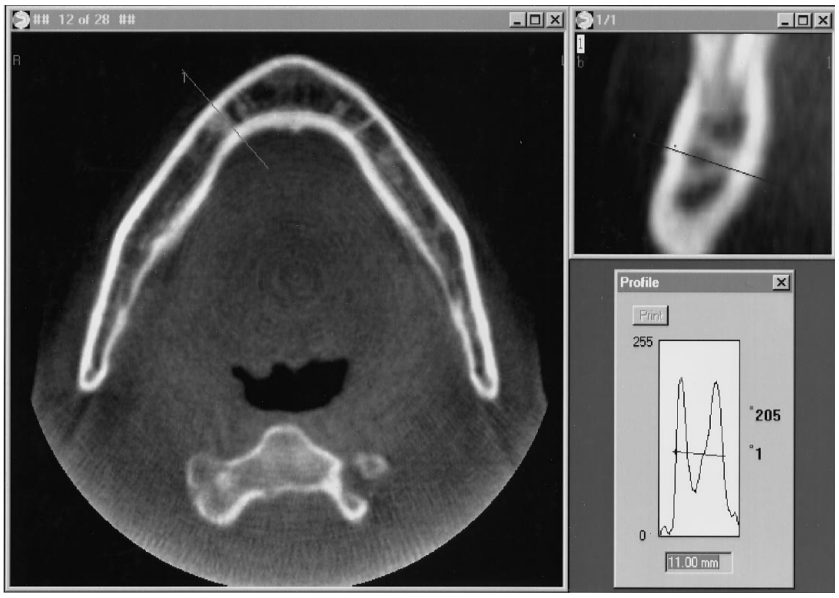

Fig. 9. Perpendicular-to-dental-arch image of the mandible with the tilted image of reference and gray-level profile along the segment showed in the PDA image. Numbers on the right side of the profile are the maximum and minimum values of gray levels; distance (in millimeters) at the base of the profile is automatically set by the software in correspondence to the bone's edges

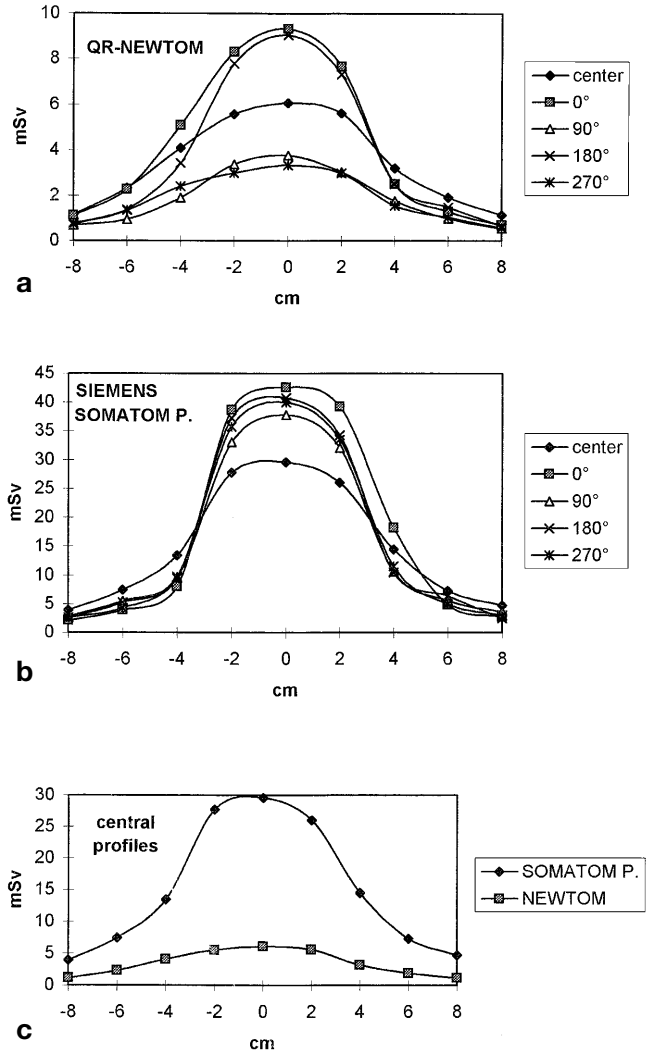

Fig. 10 a–c. Radiation dose profiles measured with the dosimetric phantom on **a** NewTom and **b** Siemens Somatom Plus 4 (Siemens, Erlangen, Germany). **c** Also reported is the comparison between the central profiles of the two machines

dose profiles (the central one and the four peripherals) allowed by the phantom are evaluated. The position along each profile has been evaluated related to the central axial plane; the latter is defined by the axis of symmetry of the beam for the NewTom, by the central slice of the scanned volume in the case of the traditional CT.

The dose profiles achieved with both the QR NewTom and Siemens Somatom Plus 4 machines are reported in Fig. 10 a and b, respectively. Figure 10 c shows, in comparison, the profiles of central doses obtained with the two machines. The precision of the considered dose values is 2 %.

The asymmetry found in the peripheral dose profiles on the NewTom (Quantitative Radiology, Verona, Italy) can be attributed to the AEC system which reduces the intensity of the X-ray beam in connection with the latero-lateral (LL) projections of the patient (angles: 90 and 270 °).

By the maximum value of the central profiles, the dose provided by the NewTom machine was approximately one sixth that by the Siemens Somatom Plus 4 machine.

The lower absorbed dose in the new CT machine is explained partially by the slightly higher level of accepted noise in the images (which limits the low-contrast resolution but not the high-contrast resolution and therefore the bony detail assessment, which is more important in the specific application), partially by the absence of the problem of the "dose profiles" overlapping which is characteristic of the traditional CT machines (mainly at low slice thickness), and partially by the use of the AEC system, which permits the modulation of the beam intensity and its setting to the minimum value compatible with the dimensions of the traversed tissues. This last option has been shown to reduce the dose by 50 % on average.

Conclusion

The growing demand for imaging of the dental and maxillo-facial structures, especially for implant treatment planning, justifies the manufacturing of specialized low-cost CT machines. The preliminary results confirm, in this respect, the advantages of the new tested tomograph. The image quality appears sufficient for the specific diagnostic needs. The geometric accuracy is also good. Moreover, the scan time is very short and the absorbed radiation dose is significantly low. These features, added to the cost-effectiveness (cost is lower than US$150,000) and easy use of the machine, make it suitable to be used also in minor diagnostic centers.

References

1. Ames JR, Johnson RP, Stevens EA (1980) Computerized tomography in oral and maxillofacial surgery. J Oral Surg 38: 145
2. Rothman SLG, Chaftez N, Rhodes ML, Schwartz MS (1988) CT in the preoperative assessment of the mandible and maxilla for endosseous implant surgery. Radiology 168: 171
3. Weinberg LA (1993) CT scan as radiologic database for optimum implant orientation. J Prosthet Dent 69: 381
4. Sethi A (1993) Precise site location for implants using CT scans: a technical note. Int J Oral Maxillofac Implants 8: 433
5. Falk A, Gielen S, Heuser L (1995) CT data acquisition as a basis for modern diagnosis and therapy in maxillofacial surgery. Int J Oral Maxillofac Surg 24: 69
6. Baily NA, Keller RA, Jacowatz CW, Kak AC (1976) The capability of fluoroscopic systems for the production of computerized axial tomograms. Invest Radiol 11: 434
7. Harrison RM, Farmer FT (1978) The determination of anatomical cross sections using a radiotherapy simulator. Br J Radiol 59: 448
8. Arnot RN, Willetts RJ, Batten JR, Orr JS (1984) Investigations using an X-ray image intensifier and a TV camera for imaging transverse sections in humans. Br J Radiol 57: 47
9. Cho PS, Johnson RH, Griffin TW (1995) Cone-beam CT for radiotherapy applications. Phys Med Biol 40: 1863
10. Saint-Félix D, Trousset Y, Picard C, Ponchut C, Roméas R, Rougée A (1994) In vivo evaluation of a new system for 3D computerized angiography. Phys Med Biol 39: 583
11. Machin K, Webb S (1994) Cone-beam X-ray microtomography of small specimens. Phys Med Biol 39: 1639
12. Motz JW, Dick CE (1975) X-ray scatter background signals in transmission radiography. Med Phys 2: 259
13. Lehr JL (1983) Truncated-view artifacts: clinical importance on CT. AJR 141: 183
14. Neitzel U (1992) Grids or air gaps for scatter reduction in digital radiography: a model calculation. Med Phys 19: 475
15. Feldkamp LA, Davis LC, Kress JW (1984) Practical cone-beam algorithm. J Opt Soc Am A 1: 612